Histol Histopathol (2016) 31: 1079-1087

http://www.hh.um.es

Histology and Histopathology

From Cell Biology to Tissue Engineering

# Immunoreactions for P53 isoforms are associated with ultrastructural proliferative profiles in benign thyroid nodules

**Maria Concetta Trovato[1,2], Rosaria Maddalena Ruggeri[1], Marco Scardigno[2], Giacomo Sturniolo[1], Roberto Vita[1], Enrica Vitarelli[2], Grazia Arena[2], Orazio Gambadoro[2], Giovanni Sturniolo[2], Francesco Trimarchi[1], Salvatore Benvenga[1], Jean-Christophe Bourdon[3] and Vittorio Cavallari[2,4]**

[1]Department of Clinical and Experimental Medicine, [2]Department of Human Pathology of the Adult and Development, University of Messina, Messina, Italy, [3]Division of Cancer Research Jacqui Wood Cancer Centre, University of Dundee, Dundee, UK and [4]Interdepartmental program of Ultrastructural Integrated Diagnostic, AOU "G. Martino", Messina, Italy

**Summary.** Background: P53 isoforms originate from the alternative initiation of P53 gene translation through usage of an internal promoter located in intron 4. All P53 isoforms are spliced in intron 9 and may modulate cell proliferation and cell fate outcome in response to DNA damage.

Aim: To examine immunoexpression of P53 isoforms in benign proliferative lesions occurring in multinodular thyroids and to assess the ultrastructural phenotype of P53 distribution in the thyrocytes of those lesions by electron microscopy.

Materials and Methods: By immunohistochemistry and transmission electron microscopy (TEM), we evaluated 38 multinodular thyroids containing a total of 102 benign lesions: 38 nodular goiters (NG; colloid=20, parenchymatous=18), 52 follicular adenomas (FA) and 12 Hashimoto's thyroditis (HT). FA were classified into 10 normo-follicular, 9 macro-follicular, 28 micro-follicular and 5 solid variants.

Results: Immunoreaction for P53 isoforms was observed in approximately 50% of all lesions, except macrofollicular variant FA (33%). At TEM analysis, immunoreactive NG, FA and TH lesions showed signs of proliferation by simultaneous appearance of dispersed chromatin, increased amounts of cytoplasmic organelles and dilation of the rough endoplasmic reticulum. TEM signs of apoptosis and proliferation were also detected in FA, but with different rates compared to NG.

Conclusion: The immunohistochemical expression of P53 isoforms in NG, FA and HT suggests their role in the development of these lesions. Ultrastructural findings support the hypothesis that P53 immuno-expression correlates with reactive proliferative changes in thyrocytes.

**Key words:** P53 isoforms, P53, Immunohistochemistry, Transmission electron microscopy, Ultrastructure, Apoptotic subcellular phenotypes, Proliferating subcellular profiles

*Offprint requests to:* Maria Trovato, MD, PhD, and Rosaria Maddalena Ruggeri, MD, PhD, Dipartimento di Patologia Umana and Dipartimento di Medicina Clinica e Sperimentale, AOU Policlinico Universitario "G. Martino", via Consolare Valeria, 1 - 98125 Messina, Italy. e-mail: mariatrovato@tin.it or mruggeri@unime.it

DOI: 10.14670/HH-11-736

## Introduction

Tumor protein 53 (TP53) is a 53 kD protein working as a transcription factor and is indicated as "the guardian of the genome" because of its contribution in maintaining genetic stability (Levine et al., 2011). This function is mainly due to the TP53 ability to control the rate of proliferation of damaged cells through the regulation of genes involved in cell-cycle arrest, DNA repair and apoptosis (Vousden and Lane, 2007).

Human TP53 gene is a 20 Kb DNA sequence located on the short arm of chromosome 17 at 13.1 locus and consists of 11 exons separated from 10 introns (Isobe et al., 1986; Pavletich et al., 1993). Bourdon and coworkers

showed that different transcripts generate from the P53 gene. The underlying molecular mechanisms are alternative initiation of translation, by usage of an internal promoter, and alternative splicing (Khoury and Bourdon, 2010). Of the two P53 gene promoter sites, the proximal (P1) is located in exon 1 and the distal (P2) is inside exon 4 (Tuck and Crawford, 1989; Marcel et al., 2010). The usage of P1 generates full-length TP53 or FLp53 and Δ40 transcripts, whereas the usage of P2 generates Δ133 and Δ160 forms (Fujita et al., 2009 Marcel et al., 2010, 2012). Furthermore, a complete elimination of three splicing sites that have been identified in intron 9 generates α transcripts, while their partial stripping results in generation of β or γ forms (Khouri and Bourdon, 2011).

To date, 12 distinct transcripts of the human TP53 gene and corresponding protein isoforms have been identified: FLP53, P53β, P53γ, Δ40α, Δ40β, Δ40γ, Δ133α, Δ133β, Δ133γ, Δ160α, Δ160β and Δ160γ, respectively (Surget et al., 2014). Orthodox FLP53 protein includes 393 amino acids (aa) that can be divided into five major functional domains. These are the amino terminal domain, consisting of two transactivation domains (TAD1, aa 1-40 and TAD2, aa 41-62), a proline-rich site (PXXP, aa 63-94), a DNA-binding domain (DBD, aa 95-290), a nuclear localization signal domain (NLS, aa 291-325) and the carboxy-terminal oligomerization domain including an oligomerization (OD, aa 326-357) and a negative-regulation site (Neg, aa 358-393) (Flaman et al., 1996; Levine et al., 2011). Since P53 isoforms contain aa 160 through 325, (Khoury and Bourdon, 2011) all P53 isoforms have a partial DBD but an intact NLS, and are able to shuttle between the cytoplasm and the nucleus (Courtois et al., 2002).

The subcellular localization of three P53 isoforms is tissue-dependent. At a subcellular level, P53 α and β isoforms are localized mainly in the nucleus and minimally in the cytoplasm, whereas P53 γ isoforms are localized both in the nucleus and cytoplasm (Bourdon et al., 2009; Khoury and Bourdon, 2011). P53 isoforms act in a tissue-specific mode through the modulation of p53 transcriptional activity and trigger the transcription of target genes involved in cell proliferation and apoptosis (Aoubala et al., 2011; Khoury and Bourdon, 2011). Among Δ133 isoforms, only the α form has been clearly associated with cell proliferation and cell fate (Aoubala et al., 2011). This isoform prevents apoptosis and replicative senescence and promotes cell proliferation in human normal fibroblast cells (Chen et al., 2009; Fujita et al., 2009; Khoury and Bourdon, 2011). Instead, the biological activities of β and γ isoforms remain ambiguous (Fujita et al., 2009). Expression of P53 isoforms has been reported in different malignancies, such as breast cancer, head and neck tumors, ovarian, renal and colon carcinomas (Bourdon et al., 2005; Boldrup et al., 2007; Marabese et al., 2008; Song et al., 2009; Fujita et al., 2009). However, the α forms have been detected in benign and precancerous lesions such as gastric inflammation by Helicobacter pylori infection and colon adenomas (Wei et al., 2012; Fujita et al., 2009).

To date, no report has investigated the distribution of P53 isoforms in thyroid lesions and its relationship between expression of these isoforms and proliferative and apoptosis status of thyrocytes. Our aims were to study the expression of P53 isoforms in benign lesions occurring in multinodular thyroids and to correlate these expressions with their ultrastructural phenotypes.

## Materials and methods

### *Patients and tissue collection*

A total of 38 multinodular thyroid glands, surgically removed and collected at the Unit of Integrated Ultrastructural Pathology, Department of Human Pathology, University of Messina were examined. The surgical samples were from patients who were diagnosed and followed up at our Endocrine Unit. All patients (30 females and 8 males, aged 32 to 71 years, mean 54.8±10.8 years) were euthyroid at time of thyroidectomy.

The 38 thyroid glands examined showed, as a common trait, a goitrous appearance associated with one single lesion in 12 cases, and with more than one in the remaining 26 cases. A total number of 102 lesions were analyzed, consisting of 38 goitres (TG), 52 follicular adenomas (FA) and 12 oncocytic hyperplasias associated with Hashimoto's thyroiditis (TH).

The clinical and pathological features of lesions are listed in Table 1. According to standard criteria of the Armed Forces Institute of Pathology (Rosai et al., 1990), the 38 goitres were classified as colloid (n=20) and parenchymatous (n=18), while the 52 FA included four variants; normofollicular (n=10), macrofollicular (n=9), microfollicular (n=28) and solid (n=5).

Each lesion sample was treated separately for immunohistochemistry and ultrastructural analysis. Thyroid tissues were fixed in 4% neutral buffered formalin and embedded in paraffin. Serial sections of each lesion were stained with hematoxylin and eosin (H&E) and Periodic acid Schiff (PAS) histochemical

**Table 1.** Clinical and histopathological features of multinodular thyroid glands.

| Clinical features | | Histopathological features | |
|---|---|---|---|
| 38 multinodular thyroids | | 102 lesions | |
| 12 Goiter plus | 1 Adenoma | 38 Goiters | 20 Colloid |
| | | | 18 Parenchymatous |
| 14 Goiter plus | 2 Adenomas | 52 Follicular Adenomas | 10 Normofollicular |
| | | | 9 Macrofollicular |
| 12 Goiters plus | 1 Adenoma | | 28 Microfollicular |
| | 1 Hashimoto's thyroiditis | | 5 Solid |
| | | 12 Hashimoto's thyroiditis | |

staining, and the slides were reviewed to confirm diagnosis.

For ultrastructural investigations, thyroid tissue samples were pre-fixed, by immersion for 12 h at 4°C, in modified Karnovsky fixative containing 2% glutaraldehyde and 2% paraformaldehyde. Next, small tissue blocks were post-fixed in 2% buffered osmium tetroxide solution, rinsed in phosphate buffer for at least 3 h, dehydrated in scalar dilutions of ethanol and embedded in epoxy resin. One micrometer thick sections were cut with diamond knives, stained with toluidine blue and observed with a light microscope. 300-400 Thick sections were obtained with diamond knives, stained with uranyl acetate and lead citrate, and then observed under a Philips EM 300 electron microscope.

### *Immunohistochemical procedure*

Immunohistochemical staining was carried out on 5-μm thick sections of the selected blocks. Two distinct monoclonal mouse antibodies were used to detect P53 and its isoforms. The former recognizes an epitope located in P53 TAD1 region, between amino acids 20-25, and reacts with FLp53, P53β and γ (DO-7, 1:100; DAKO, Carpinteria, CA, USA); the latter antibody recognizes an epitope located within the P53 DBD region, between amino acids 181-190, and binds the full set of P53 isoforms (DO-11, working dilution 1:500; Novus Biologicals Europe, Cambridge, UK; www.novusbio.com/NB100-65557).

Antigen retrieval technique was carried out as described by Gown et al. (1993). Tissue sections were deparaffinized in xylene and rehydrated in alcohol. Then, the endogenous biotin was inactivated by addition of 0.05% (v/v) solution of streptavidin in phosphate-buffered saline (PBS) and endogenous peroxidase activity was quenched by adding 0.3% (v/v) solution of 3% $H_2O_2$/methanol for 30 min. Immunostaining was obtained with the LSAB system (Universal Dako LSAB® + Kit, Peroxidase, Carpinteria, CA, USA) by using an automated slide processing system designed by Autostainer Link 48 system (Dako). Reaction was visualized using 3.3'-diaminobenzidine (Dako) activated with 0.05% hydrogen peroxide. Sections were counterstained with Mayer's haematoxylin, dehydrated and mounted. Specificity of the binding was assessed on appropriate negative controls, either by omitting the primary antiserum or by replacing the primary antiserum with normal mouse serum. In addition, an immunoabsorption test was performed to confirm the specific immunoreactivity of the antibody.

Specimens of breast carcinoma were used as appropriate positive controls for both P53 antibodies. P53 and P53 isoforms immunoreactions were estimated using the following criteria: (i) number of positive cases; (ii) number of reactive epithelial cells per case: count of the number of reactive cells was based on evaluation of 1000 cells/case, using 40x magnification; (iii) subcellular location of the staining: cytoplasm and nucleus; (iv) semiquantitative grading of staining using a "Quickscore" method as proposed by Detre et al. (Detre et al., 1995). This method was based either on the proportions of immunostained cells or on the intensity of labelling. The immunostained cells were scored on a system from I to IV (I=0-4% of cells; II=5-19%; III=20-39%; IV=40-59%). The intensity of immunostaining was graded from 0 to 3, corresponding with absence of labelling, weak, intermediate, and strong immunostaining, respectively. Grade I of immunoreactions was considered as unreactive; grade II of stained cells plus grade 2 or 3 of stain was indicated as class A; grade III plus grade 2 or 3 was recorded as class B; grade VI plus grade 2 or 3 was indicated as class C.

Histological and immunohistochemical evaluations were carried out blindly by three different pathologists (M.T., M.S. and V.C.) with an inter-observer concordance of nearly 100%. Minimal inter-observer discrepancies were overcome by mean value.

### *Ultrastructural evaluation*

We considered two different phenotypes that correspond to the apoptotic or the proliferative status of follicular cells. The two cell phenotypes were defined by five criteria, of which two evaluate the nuclear compartment and three the subcellular structures of cytoplasm. The nuclear parameters evaluated were the border of the nuclear membrane (catalogued as regular or irregular) and chromatin (catalogued as densely packed or dispersed). In the cytoplasm, the profile of cell basal borders (regular or irregular), the number of organelles such as mitochondria, lysosomes, phagolysosomes (in comparison to the corresponding number in normal thyrocytes) and the status of rough endoplasmic reticulum (RER) (dilated or non-dilated) were considered.

### *Statistical analysis*

Immunohistochemical and ultrastructural data were tested for normal distribution and variance (mean ± standard deviation) and analyzed by the $\chi^2$ test with Yates' correction for continuity and the two-tailed Student's t-test, respectively. Statistical analyses were performed using SPSS 11.0 for Window package. The level of statistical significance was set at $P<0.05$.

## Results

### *Immunohistochemistry*

Immunohistochemistry features are shown in Figs. 1, 2. All reactive samples for DO-7 showed DO-11 immunostaining. However, DO-7 immunoreaction was mainly located in the nucleus while DO-11 staining

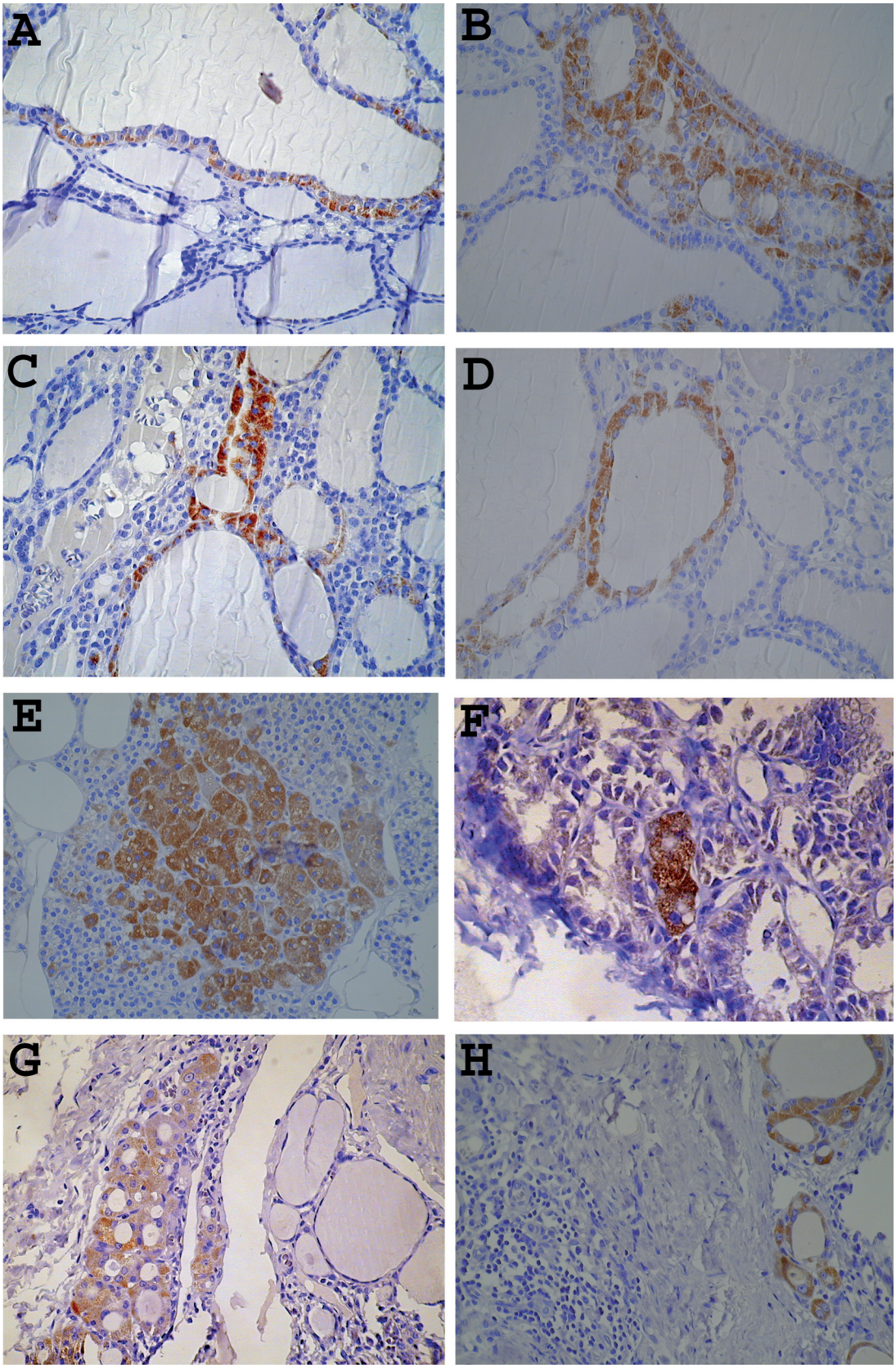


**Fig. 1.** Immunoreactions of P53 isoforms in goitrous lesions, follicular adenoma and Hashimoto's thyroditis. **A.** Immunoreactivity in a colloid goiter catalogued as class A (that is, 5-19% of stained cells plus intermediate or strong immunostaining as specified in Material and Methods). **B, C, D.** Class A immunoreactions in parenchymatous goiter, normofollicular and macrofollicular adenomas, respectively. **E.** Class B immunoreaction (20-39% of stained cells plus intermediate or strong immunostaining) appearing in a microfollicular adenoma. **F, G, H.** Class A immunoreactions observed in solid adenoma and Hashimoto's thyroditis. In Panel **G**, note that immunostaining is located in Hürthle cells. A-E, G, H, x 200; F, x 400

appeared in both cytoplasmatic and nuclear compartments.

Immunoreactivities for FLP53, P53β and γ were observed with a frequency near to 7% of multinodular glands, showing one or two adenomas and absence of HT (Table 2A). There were only three immunostained lesions and they involved parenchimatous goiter, microfollicular and solid FA groups, respectively (Table 2B and C). In all reactive cases immunostainings conceivable with class A score (Table 3) were detected.

In sharp contrast, immunoreactions for P53 isoforms were detected with a frequency of 50-60%, regardless of number (one or two) of FA (Table 2A) and the nature (goitre, FA, HT) of the lesions (Table 2B). However, of the four FA histological subtypes, the macrofollicular subtype had the lowest frequency (33%) (Table 2C), but was not statistically different from the frequencies of other subtypes (Df= 3, $\chi^2$= 1.70, P= 0.64).

Much variation among lesions was observed when they were categorized into the four Quickscore based classes (Table 3). While no lesion fell into the D category, three lesions (colloid goiter, normofollicular adenoma and macrofollicular adenoma) belonged to the C class only. The other lesions belonged both to class A

**Table 2.** Immunoreactivity for P53 and isoforms in benign lesions of multinodular thyroids.

| | DO-7 | | DO-11 | |
|---|---|---|---|---|
| | Reactive (% of cases) | Unreactive (% of cases) | Reactive (% of cases) | Unreactive (% of cases) |
| A Multinodular thyroids | | | | |
| Goiter plus 1 Adenoma | 8 | 92 | 58 | 42 |
| Goiter plus 2 Adenomas | 7 | 93 | 57 | 43 |
| Goiter plus 1 Adenoma plus Hashimoto's thyroditis | 0 | 100 | 50 | 50 |
| B Pathological lesions | | | | |
| Goiter | 3 | 97 | 58 | 42 |
| Adenoma | 4 | 96 | 52 | 48 |
| Hashimoto's thyroditis | 0 | 100 | 58 | 42 |
| C Histo-pathological lesions | | | | |
| Colloid goiter | 0 | 100 | 60 | 40 |
| Parenchymatous goiter | 5 | 95 | 56 | 44 |
| Normofollicular adenoma | 0 | 100 | 50 | 50 |
| Macrofollicular adenoma | 0 | 100 | 33 | 67 |
| Microfollicular adenoma | 3 | 43 | 57 | 43 |
| Solid adenoma | 20 | 80 | 60 | 40 |
| Hashimoto's thyroditis | 0 | 100 | 58 | 42 |

Immunohistochemistry was performed using two distinct monoclonal antibodies (DO-7 and DO-11) directed against different epitopes of P53 and its isoforms, as specified under Materials and Methods.

**Table 3.** Cellular distribution of immunostaining for Δ 133 isoforms of P53 in immunoreactive lesions.

| | DO-7 | | | DO-11 | | |
|---|---|---|---|---|---|---|
| | A* (% of cases) | B** (% of cases) | C*** (% of cases) | A* (% of cases) | B** (% of cases) | C*** (% of cases) |
| Colloid goiter | 0 | 0 | 0 | 100 | 0 | 0 |
| Parenchymatous goiter | 100 | 0 | 0 | 70 | 30 | 0 |
| Normofollicular adenoma | 0 | 0 | 0 | 100 | 0 | 0 |
| Macrofollicular adenoma | 0 | 0 | 0 | 100 | 0 | 0 |
| Microfollicular adenoma | 100 | 0 | 0 | 44 | 31 | 25 |
| Solid adenoma | 100 | 0 | 0 | 67 | 33 | 0 |
| Hashimoto's thyroditis | 0 | 0 | 0 | 57 | 43 | 0 |

Immunohistochemistry was performed using two distinct monoclonal antibodies (DO-7 and DO-11) directed against different epitopes of P53 and its isoforms, as specified under Materials and Methods. The immunoreactivities for Δ 133 isoforms of P53 were classified as Class A, B, C and D by using "Quickscore" method as proposed by Detre et al. (1995) and scoring the intensity of labelling. Both the proportion of immunostained cells and the intensity of labelling were evaluated. Score of stained cells was assessed in a system from I to VI (I = 0-4% of cells; II = 5-19%; III = 20-39%; IV = 40-59%; V = 60-79%; VI = 80-100%). Intensity of immunostaining was scored from 0 to 3 (absent, weak, intermediate, and strong immunostaining, respectively). *Class A was grade II of immunostained cells plus grade 2 or 3 of immunostaining; **class B corresponded with grade III plus grade 2 or 3; *** class C was grade IV plus grade 2 or 3.

(with a variation in rate from 44% for the microfollicular subtype of FA to 70% for the parenchymatous goiter) and class B (with a smaller variation, that is, 30-43%). The macrofollicular subtype of FA was the only lesion to be distributed among three classes.

### *Ultrastructural phenotypes*

Ultrastructural subcellular structures of both apoptotic and proliferating phenotypes are summarized in Table 4, and illustrated in Fig. 3.

The apoptotic phenotype was recognized in thyrocytes showing the following ultrastructural criteria: irregular borders of both nuclear and cytoplasm membranes, densely packed chromatin in nucleus, normal amounts of organelles in cytoplasm and no dilatation of RER. In contrast, the proliferative phenotype was recognized in thyrocytes showing regular profiles of both the nuclear and cytoplasmic basal borders, dispersed chromatin, increasing amounts of cytoplasmic organelles and dilatation of RER.

Positive immunoreactions of P53 isoforms occurring in goiters could be associated with ultrastructural proliferative phenotype as three out of five ultrastructural criteria indicated a proliferative status in the follicular cells. Indeed, in 100% of reactive goitrous nodules chromatin was dispersed, the amount of organelles was increased and RER was dilated (Table 4). At least for the first two of these three apoptotic ultrastructural characteristics, rates were 25% and 25% in the group of goiters that did not express P53 isoforms (Table 4).

FA expressing P53 isoforms exhibited ultrastructural features associated with proliferation, but at lower rates compared to goiters. Only in 67% of immunostained FA were dispersed chromatin, increase of organelles and dilated RER (100% vs 67%; $\chi^2$=37.16; P<0.05) detected simultaneously (Table 4). Even unstained FA displayed ultrastructural features and that fitted both the apoptosis and the proliferation phenotype, but criteria indicating apoptosis or proliferation of follicular cells in FA differed from those of goiters. In particular, 80% of unreactive FA had dispersed chromatin (a proliferative feature), while 88% had irregular cytoplamic borders and 64% irregular nuclear borders (both irregularities indicating apoptosis) (Table 4).

In immunoreactive HT, ultrastructural phenotype was associated with proliferation and was similar to that of immunostained FA as most or all of them showed dispersed chromatin (71%), increased amounts of organelles (100%) and dilatation of RER (100%) (Table 4). Unreactive HT also showed mainly an ultrastructural proliferative profile, since in 100% of cases the membranous nuclear borders were regular, amounts of organelles were increased and RER was dilated. However, unstained HT also displayed ultrastructural features associated with the apoptotic phenotype, such as densely packed chromatin (60%) and irregular cytoplasmatic borders (100%) (Table 4).

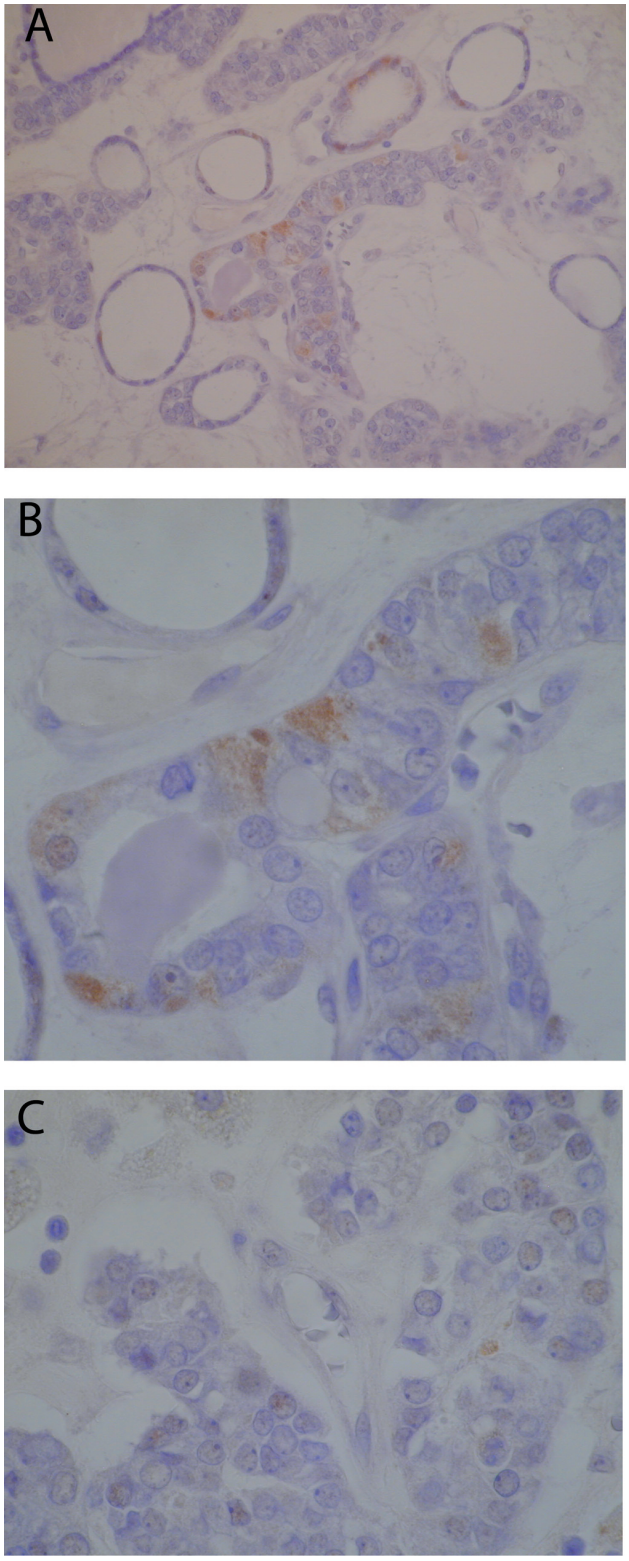


**Fig. 2.** Immunoreactions of P53 in goitrous lesion and follicular ademomas. **A.** Immunoreactivity in a parenchymatous goiter catalogued as class A (5-19% of stained cells plus intermediate or strong immunostaining as specified in Material and Methods). **B and C.** Class A immunoreactions in microfollicular and solid adenomas, respectively. A, x 200; B, C, x 400

## Discussion

The thyroid may host two or more nodules simultaneously that have different biological behaviour. For instance, the same gland may be occupied by several benign nodules or by benign nodule(s) coexisting with cancerous nodule(s). The majority of thyroid nodules are benign, and most of them are classified as goiters, FA and HT (American Thyroid Association (ATA) Guidelines Taskforce on Thyroid Nodules and Differentiated Thyroid Cancer, 2009). To this time, different studies were performed for discrimination of benign from malignant thyroid lesions (Eroz et al., 2013a,b; Oktay et al., 2015). In benign nodules of multinodular thyroids, expressions of different growth factors have been reported, such as HGF and interleukin 6 to indicate their involvement in either proliferation or apoptosis to balance the nodular growth (Ruggeri et al., 2006, 2007; Sarlis and Benvenga, 2004).

The role of P53 isoforms in thyroid glands remains unclear, their distribution on thyroid tissues has not been assessed, and any investigation has correlated their role with proliferation and apoptosis occurring in follicular lesions (Malaguarnera et al., 2007; Marcello, 2013; Surget et al., 2014). We have addressed our efforts to evaluate these isoforms in multinodular thyroid glands showing benign lesions, only, by studying also ultrastructural alteration linked to proliferation or apoptosis.

The first objective of our research was to verify if the expressions of P53 isoforms could be associated with the number of benign nodules occurring simultaneously in thyroid tissues and we excluded this association. Secondly, we evaluated if these isoforms could be expressed differently in the different benign lesions occurring in multinodular thyroids. We have found that

**Table 4.** Ultrastructural subcellular phenotypes of benign thyroid lesions subdivided into DO-11 reactive and unreactive lesions.

| | Reactive (% of cases) | | | | | | | | Unreactive (% of cases) | | | | | | | |
|---|---|---|---|---|---|---|---|---|---|---|---|---|---|---|---|---|
| | Nuclear borders | | Chromatin | | Citoplasmatic borders | | Organelles | RER | Nuclear borders | | Chromatin | | Citoplasmatic borders | | Organelles | RER |
| DO-11 | Regular | Irregular | Densely packed | Disperse | Regular | Irregular | Increased | Dilated | Regular | Irregular | Densely | Disperse packed | Regular | Irregular | Increased | Dilated |
| Goiters | 9 | 91 | 0 | 100 | 0 | 100 | 100 | 100 | 75 | 25 | 75 | 25 | 41 | 59 | 25 | 100 |
| Adenomas | 7 | 93 | 7 | 93 | 48 | 52 | 96 | 67 | 36 | 64 | 20 | 80 | 12 | 88 | 48 | 48 |
| Hashimoto's thyroditis | 14 | 86 | 29 | 71 | 43 | 57 | 100 | 100 | 100 | 0 | 60 | 40 | 0 | 100 | 100 | 100 |

*The monoclonal antibody DO-11 recognizes an epitope located within the P53 DBD region, between amino acids 181-190, and binds the full set of P53 isoforms, as specified under Material and Methods.

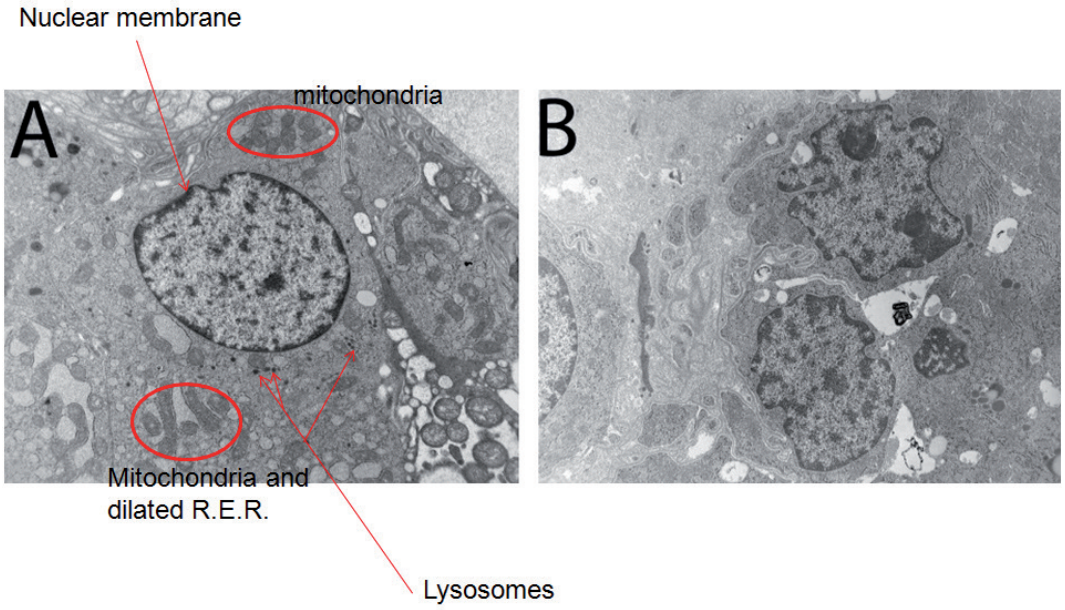


**Fig. 3.** Ultrastructural findings of reactive and unreactive lesions for Δ 133 isoforms of P53. **A.** Ultrastructural features of thyrocites pertaining to an FA immunostained by Δ 133 isoforms of P53. To note: the simultaneous appearance of dispersed chromatin, dilated RER and increase of organelles. **B.** Ultrastructural features of thyrocites pertaining to an FA unreactive to Δ 133 isoforms of P53. To note: the combination of densely packed chromatin and irregular cytoplasmatic borders. High-magnification TEM image.

when benign lesions are subdivided into histological subtypes (or variants) significant differences among variants can be detected. Thus, the tendency to express those isoforms is scarce in the macrofollicular variant of FA but is high in parenchymatous goiters, as well as in microfollicular and solid FA variants.

Altogether, these data indicate that in multinodular thyroids the immunoexpression of P53 isoforms differs among different histological variants of benign lesions. In addition, this expression is associated with a cell population and colloid content, since the number of follicular cells increases and colloid content decreases moving from macrofollicular to normofollicular, microfollicular or solid histological variants of FA.

Lastly, we tried to correlate immunoreactions for P53 isoforms with apoptotic and proliferative ultrastructural phenotypes. Mainly, our results have demonstrated that immunoreactive lesions displayed subcellular features which differ from unreactive ones. Specifically, in reactive lesions three ultrastructural features fitting with cellular proliferation appeared simultaneously. On the contrary, in unreactive lesions subcellular characteristics more conceivable with follicular apoptosis occurred. Additionally, we observed a major incidence of proliferative phenotypes in reactive goitrous lesions compared to FA and HT.

These results indicate that simultaneous ultrastuctural features depicting dispersed chromatin, dilated RER and increase of organelles in cytoplasm are associated with immunoexpressions of P53 isoforms as, in the presence of these immunoreactions, those three features appear simultaneously. Indeed, the different incidence of proliferative phenotype detected among P53 isoform reactive lesions may be referable to a different status of proliferation of lesions.

Considering that P53 isoforms appear in benign histotypes with ultrastructural proliferative profile, our investigations may have practice relapses in diagnostic fields to select proliferating benign lesions. This is because the combination of P53 immunoreactions and ultrastructural proliferative features mark proliferating subtypes of goiters, FA and HT. Therefore, an alliance between these two procedures may be proposed as a reasonable tool to distinguish benign proliferating subtypes in histological diagnostic procedures to identify benign lesions with active proliferating follicular cells.

## References

American Thyroid Association (ATA) Guidelines Taskforce on Thyroid Nodules and Differentiated Thyroid Cancer, Cooper D.S., Doherty G.M., Haugen B.R., Kloos R.T., Lee S.L., Mandel S.J., Mazzaferri E.L., McIver B., Pacini F., Schlumberger M., Sherman S.I., Steward D.L. and Tuttle R.M. (2009). Revised American Thyroid Association management guidelines for patients with thyroid nodules and differentiated thyroid cancer. Thyroid 19, 1167-1214.

Aoubala M., Murray-Zmijewski F., Khoury M.P., Fernandes K., Perrier S., Bernard H., Prats A.C., Lane D.P. and Bourdon J.C. (2011). P53 directly transactivates Delta133p53alpha, regulating cell fate outcome in response to DNA damage. Cell. Death Differ. 18, 248-258.

Boldrup L., Bourdon J.C., Coates P.J., Sjöström B. and Nylander K. (2007). Expression of p53 isoforms in squamous cell carcinoma of the head and neck. Eur. J. Cancer 43, 617-623.

Bourdon J.C., Fernandes K., Murray-Zmijewski F., Liu G., Diot A., Xirodimas D.P., Saville M.K. and Lane D.P. (2005). p53 isoforms can regulate p53 transcriptional activity. Genes Dev. 19, 2122-2137.

Chen J., Ng S.M., Chang C., Zhang Z., Bourdon J.C., Lane D.P. and Peng J. (2009). p53 isoform delta113p53 is a p53 target gene that antagonizes p53 apoptotic activity via BclxL activation in zebrafish. Genes Dev. 23, 278-290.

Courtois S., Verhaegh G., North S., Luciani M.G., Lassus P., Hibner U., Oren M. and Hainaut P. (2002). DeltaN-p53, a natural isoform of p53 lacking the first transactivation domain, counteracts growth suppression by wild-type p53. Oncogene 21, 6722-6728.

Detre S., Saclani Jotti G. and Dowsett M. (1995). A "quickscore" method for immunohistochemical semiquantitation: validation for oestrogen receptor in breast carcinomas. J. Clin. Pathol. 48, 876-878.

Eröz R., Unluhizarci K., Cucer N. and Ozturk F. (2013a). Value of argyrophilic nucleolar organizing region protein determinations in nondiagnostic fine needle aspiration samples (due to insufficient cell groups) of thyroid nodules. Anal. Quant. Cytopathol. Histopathol. 35, 226-231.

Eroz R., Cucer N., Unluhizarci K. and Ozturk F. (2013b). Detection and comparison of cut-off values for total AgNOR area/nuclear area and AgNOR number/nucleus in benign thyroid nodules and normal thyroid tissue. Cell Biol. Int. 37, 257-261.

Flaman J.M., Waridel F., Estreicher A., Vannier A., Limacher J.M., Gilbert D., Iggo R. and Frebourg T. (1996). The human tumour suppressor gene p53 is alternatively spliced in normal cells. Oncogene 12, 813-818.

Fujita K., Mondal A.M., Horikawa I., Nguyen G.H., Kumamoto K., Sohn J.J., Bowman E.D., Mathe E.A., Schetter A.J., Pine S.R., Ji H., Vojtesek B., Bourdon J.C., Lane D.P. and Harris C.C. (2009). p53 isoforms, D133p53 and p53b, are endogenous regulators of replicative cellular senescence. Nat. Cell. Biol. 11, 1135-1142.

Gown A.M., deWever N. and Battifora H. (1993). Microwaved-based antigen unmasking. A revolutionary new technique for routeine immunohistochemistry. Appl. Immunohistochem. 1, 256-266.

Isobe M., Emanuel B.S., Givol D., Oren M. and Croce C.M. (1986). Localization of gene for human p53 tumour antigen to band 17p13. Nature. 320, 84-85.

Khoury M.P. and Bourdon J.C. (2011). p53 Isoforms: An Intracellular Microprocessor? Genes and Cancer 2, 453-465.

Khoury M.P. and Bourdon J.C. (2010). The isoforms of the p53 protein. Cold. Spring. Harb. Perspect. Biol. 2, a000927.

Levine A.J., Tomasini R., McKeon F.D., Mak T.W. and Melino G. (2011). The p53 family: guardians of maternal reproduction. Nat. Rev. Mol. Cell Biol. 12, 259-265.

Malaguarnera R., Vella V., Vigneri R. and Frasca F. (2007). P53 family proteins in thyroid cancer. Endocr. Relat. Cancer 14, 43-60.

Marabese M., Marchini S., Marrazzo E., Mariani P., Cattaneo D., Fossati R., Compagnoni A., Signorelli M., Moll U.M., Codegoni A.M. and Broggini M. (2008). Expression levels of p53 and p73 isoforms in stage I and stage III ovarian cancer. Eur. J. Cancer 44, 131-141.

Marcel V., Petit I., Murray-Zmijewski F., Goullet de Rugy T., Fernandes K., Meuray V., Diot A., Lane D.P., Aberdam D. and Bourdon J.C. (2012). Diverse p63 and p73 isoforms regulate Delta133p53

expression through modulation of the internal TP53 promoter activity. Cell. Death Differ. 19, 816-826.

Marcel V., Vijayakumar V., Fernández-Cuesta L., Hafsi H., Sagne C., Hautefeuille A., Olivier M. and Hainaut P. (2010). p53 Regulates the transcription of its Delta133p53 isoform through specific response elements contained within the TP53 P2 internal promoter. Oncogene 29, 2691-2700.

Marcello M.A., Morari E.C., Cunha L.L., De Nadai Silva A.C., Carraro D.M., Carvalho A.L., Soares F.A., Vassallo J. and Ward L.S. (2013). P53 and expression of immunological markers may identify early stage thyroid tumors. Clin. Dev. Immunol. 2013, 846584.

Oktay M., Eroz R., Oktay N.A., Erdem H., Başar F., Akyol L., Cucer N. and Bahadir A. (2015). Argyrophilic nucleolar organizing region associated protein synthesis for cytologic discrimination of follicular thyroid lesions. Biotech. Histochem. 90, 179-183.

Pavletich N.P., Chambers K.A. and Pabo C.O. (1993). The DNA-binding domain of p53 contains the four conserved regions and the major mutation hot spots. Genes Dev. 7, 2556-2564.

Rosai J., Carcangiu M.L. and De Lellis R. (1990). Tumors of the thyroid gland. In: Atlas of tumor pathology. Armed Forces Institute of Pathology, Washington DC, 19.

Ruggeri R.M., Barresi G., Sciacchitano S., Trimarchi F., Benvenga S. and Trovato M. (2006). Immunoexpression of the CD30 ligand/CD30 and IL-6/IL-6R signals in thyroid autoimmune diseases. Histol. Histopathol. 21, 249-256.

Ruggeri R.M., Sciacchitano S., Trimarchi F., Barresi G. and Trovato M. (2007). Expression of hepatocyte growth factor in Hashimoto's thyroiditis with nodular lesions. Eur. J. Histochem. 51, 193-198.

Sarlis N.J. and Benvenga S. (2004). Molecular signaling in thyroid cancer. Cancer Treat. Res.122, 237-264.

Song W., Huo S.W., Lu J.J., Liu Z., Fang X.L., Jin X.B. and Yuan M.Z. (2009). Expression of p53 isoforms in renal cell carcinoma. Chin. Med. J. Engl. 122, 921-926.

Surget S., Khoury M.P. and Bourdon J.C. (2014). Uncovering the role of p53 splice variants in human malignancy: a clinical perspective. Onco. Targets Ther. 7, 57-68.

Tuck S.P. and Crawford L. (1989). Characterization of the human p53 gene promoter. Mol. Cell. Biol. 9, 2163-2172.

Vousden K.H. and Lane D.P. (2007). p53 in health and disease. Nat. Rev. Mol. Cell. Biol. 8, 275-283.

Wei J., Noto J., Zaika E., Romero-Gallo J., Correa P., El-Rifai W., Peek R.M. and Zaika A. (2012). Pathogenic bacterium *Helicobacter pylori* alters the expression profile of p53 protein isoforms and p53 response to cellular stresses. Proc. Natl. Acad. Sci. USA109, E2543-E2550.

Accepted February 16, 2016